IEEE Access
Multidisciplinary | Rapid Review | Open Access Journal

Received December 12, 2019, accepted January 8, 2020, date of publication January 13, 2020, date of current version January 21, 2020.

Digital Object Identifier 10.1109/ACCESS.2020.2966006

Tightness Analysis of Underground Natural Gas and Oil Storage Caverns With Limit Pillar Widths in Bedded Rock Salt

NAN ZHANG[1], XILIN SHI[2], YUN ZHANG[1], AND PENGFEI SHAN[1]

[1]Key Laboratory of Western Mines and Hazard Prevention, Ministry of Education of China, College of Energy Engineering, Xi'an University of Science and Technology, Xi'an 710054, China

[2]State Key Laboratory of Geomechanics and Geotechnical Engineering, Institute of Rock and Soil Mechanics, Chinese Academy of Sciences, Wuhan 430071, China

Corresponding authors: Nan Zhang (zhangnan0032@foxmail.com) and Xilin Shi (xlshi@whrsm.ac.cn)

This work was supported in part by the National Science Foundation of China under Grant 51774266, Grant 41502296, Grant 51404241, and Grant 51404241, in part by the National Natural Science Foundation of China Innovative Research Team under Grant 51621006, in part by the Youth Innovation Promotion Association CAS under Grant 2016296, and in part by the Natural Science Foundation for Innovation Group of Hubei Province, China, under Grant 2016CFA014.

ABSTRACT To fully utilize the abandoned salt cavern resources and to increase the total amount of the fossil energy reserve of China, reconstructing some of these salt caverns for underground gas storage (UGS) or strategic petroleum reserve (SPR) would be an effective method. The salt resources in China mainly are bedded salt, which brings great challenges for the cavern construction and safety evaluation. In this paper, the investigations are presented to evaluate the tightness of the UGS and SPR salt cavern facilities, located in the bedded rock of Jintan, China. Microcosmic analysis, and permeability and porosity tests of the surrounding rock are carried out to determine their properties, which provide the basic data for the tightness assessment. A 3-D numerical model is developed based on the test results and the geological features of the target formation. The numerical simulation results show that the seepage velocity, seepage range and loss rate of leakage of the SPR salt caverns are much smaller than those of UGS salt caverns. The cavern's pillar width with a pillar to diameter ratio (P/D) of 1.5 can satisfy the tightness requirement of SPR salt caverns, but it cannot meet the requirement of UGS caverns. This indicates that some existing abandoned salt caverns in Jintan which are unsuitable for UGS due to their small pillar width have the potential to be rebuilt for SPR. This would help to increase the storage capacity of crude oil in China. The results can also provide a reference for the implementation of similar projects in other bedded salt districts.

INDEX TERMS Bedded rock salt, underground gas storage, strategic petroleum reserve, tightness, seepage.

I. INTRODUCTION

Energy has always been considered as the engine and fundamental impetus of social-economic development. The supply of energy should be ensured as continuously and reliably. With the fast development of the Chinese economy and the resulting rapid growth of energy consumption, the needs for energy are increasingly growing, especially for fossil energy, such as crude oil and natural gas [1]–[3]. Meanwhile, the growing shortage of fossil energy supply is becoming a serious problem, one of the most important issues for China's national security and environmental pollution [4]–[6]. According to the data from the National Energy Administration of China [7], as shown in FIGURE 1 (a), the total amount of crude oil reserves is 3.773×10^7 t by the end of 2017, about 29 days of the annual consumption, far less than the 90 days proposed by the International Energy Agency (IEA). The dependence on oil import of China will exceed 68% in the year 2018, much higher than the international security value (50%). Simultaneously, the natural gas storage of China is as low as 3% at the end of 2017, much less than the international level of 15% of the annual consumption, far from enough to guarantee a reliable natural gas market, as shown in FIGURE 1 (b). The main reason for these deficiencies is the shortage of sufficient and available energy storage space. Strategic petroleum

The associate editor coordinating the review of this manuscript and approving it for publication was Shuaihu Li.

This work is licensed under a Creative Commons Attribution 4.0 License. For more information, see http://creativecommons.org/licenses/by/4.0/

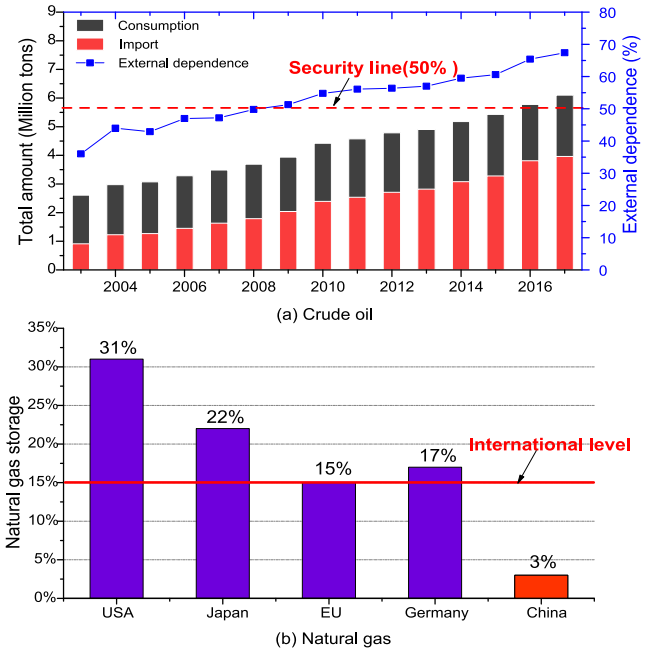

FIGURE 1. **The current reserve situation of crude oil and natural gas in China.**

reserve (SPR) is important to protect national petroleum security and blunt the significant economic impacts of a shortage stemming from international events in times of crisis [8]. Underground natural gas (UGS) storage plays a vital role in competitive natural gas markets because the average variability in the consumption of natural gas is much greater than the average variability in production [9]–[12]. Due to these reasons, the China government is promoting the construction of fossil energy storage facilities, so as to control price fluctuations, balance supply and demand, withstand emergencies and safeguard the social-economic safety.

Among all the types of energy storage, underground salt cavern storage is recognized as one of the safest methods of storing large amounts of crude oil and natural gas and has been widely used, due to the impermeability and rheology of rock salt [13]–[16]. For instance, more than 90% of the U.S. SPR is stored in salt caverns, located at four different sites in Texas and Louisiana. The total oil-storage capacity exceeds 1.19×10^8 m^3. Salt cavern gas storage represents 23% of the total natural gas underground storage. About 2×10^7 m^3 of crude oil and 1.98×10^{10} m^3 of natural gas were stored in salt caverns in Germany at the end of 2011. In central and eastern China, large rock salt resources are present and abandoned salt caverns can be constructed or rebuilt as large-scale underground energy storage facilities, e.g., the Jintan Salt Mine, Huai'an salt mine and Yunying salt mine [17]. The total volume of the abandoned salt caverns in these places is approximately 2×10^8 m^3. In recent years, it has increased at a rate of approximately 2×10^7 m^3 per year. If these abandoned salt caverns could be efficiently utilized, it would greatly increase the energy storage amount.

A number of salt caverns have been constructed for UGS in China since 2007. So far, no salt cavern has been constructed for SPR. In recent years, the government began to strongly support constructing underground storage facilities according to Phase III of China's SPR plan, especially underground SPR salt caverns. Jintan salt mine, in Jiangsu province, will be the primary construction area [18]. FIGURE 2 shows a schematic diagram of UGS and SPR salt caverns in layered salt formations. Salt caverns are deep cavities that are connected to the surface through a cased and cemented well. One to several casings is set in the well to allow injection or withdrawal of fluids into or from the cavern. The depth of the salt caverns is about 1000 m. The volume of each cavern will be designed as about 3.0×10^5 m^3.

Different from most of the SPR and UGS salt caverns worldwide, which are mainly in thick salt domes, the rock salt of China has a typical bedded structure, composed of salt layers and interlayers (e.g. anhydrite, mudstone, and glauberite) [19]–[21]. The different characteristics of rock salt and interlayers may have a significant impact on the determination of reservoir operating parameters, and even on the cavern stability and tightness [22]. Many research studies have been conducted to assess the safety and tightness of the large-scale underground energy storage facilities in bedded rock salt. Hou *et al.* [23] researched the influences of drilling on the permeability of rock salt in the excavation disturbed zone (EDZ) by laboratory experiments. They showed that the disturbance produced by drilling has a significant impact on the permeability of rock salt. Deng and Wang [24] obtained the permeability of gas reservoir caprocks and found that their permeability was larger than that of rock salt by 2-4 orders of magnitude. Staudtmeister and Rokahr [25] used the finite element method (FEM) for salt cavern dimensional analysis and stability evaluation. They gained a realistic prediction of the behavior with complex loading histories. Wei *et al.* [26] investigated the suitability of salt caverns under adverse geological conditions and showed that the mechanical properties of the bedded rock salts are satisfactory for the stability of caverns and that the permeability of the interlayers is a key factor in influencing gas seepage. Khaledi *et al.* [27] used GID software to simulate the excavation process and cyclic loading operation of a salt cavern. They identified the influence of internal pressure on the stability of surrounding rock and on the allowable operating conditions. The above research results show that the safety and tightness analysis of UGS and SPR salt caverns are complicated and problems of deep concerned. Among all the factors, to fully use the abundant salt caverns, the separation distance between caverns (pillar width) is an important factor that we consider. Van Sambeek [28] established a salt pillar design equation and pointed out that the pillar width between the salt caverns was an important index to evaluate cavern stability and tightness. The cavern design reference in America specifies that each cavern possesses a pillar to cavern diameter ratio (P/D) of 1.78 or greater. Wang *et al.* [29] used FLAC^{3D} to investigate factors affecting the allowable width for pillars

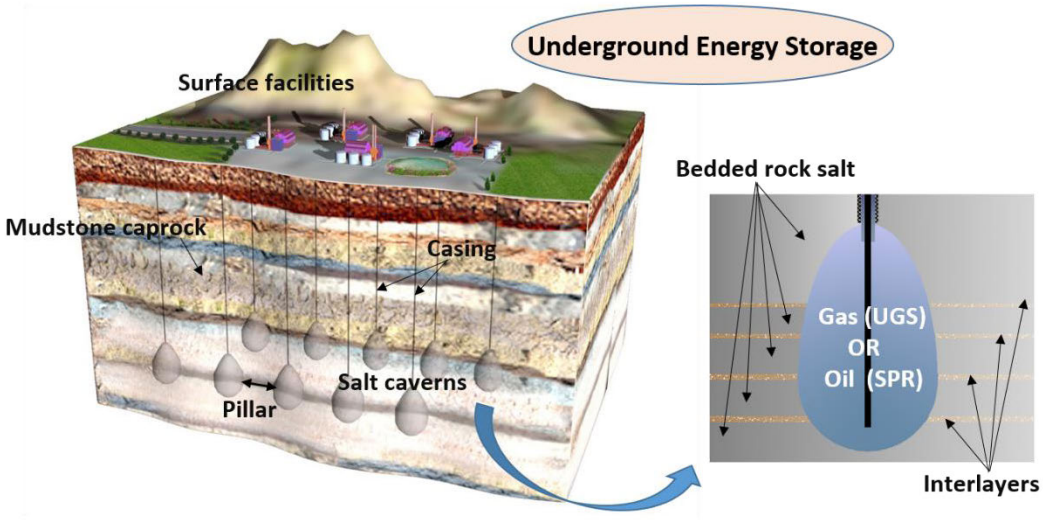

FIGURE 2. Schematic diagram of UGS and SPR salt caverns in layered salt formations in Jintan salt mine.

in bedded rock salt. They recommended that the minimum pillar width should be 2.0 times the maximum diameter of a cavern. According to this criterion, a number of abandoned salt caverns with the P/D less than 1.78-2.0 cannot be used for energy storage, resulting in a huge waste of salt resources. Actually, most of these abandoned caverns have narrow pillars, at least half of them with a P/D around 1.5. That is due to the fact that the initial purpose of these caverns was to exploit salt rather than underground energy storage. In recent years, this criterion is considered too conservative by many scholars, and a number of acquired caverns are already in violation of the criteria [30]. According to the latest Germany's design criterion, a minimum value of P/D of 1.5 is recommended. Zhang *et al.* [18] demonstrated that the pillar width of the SPR caverns with a limit pillar to diameter ratio (P/D) of 1.5 is confirmed can satisfy both the stability and availability. However, the tightness of the caverns should be further investigated. Meanwhile, the pillar to diameter ratio (P/D) of around 1.5 has not been confirmed for UGS salt caverns in bedded rock, China. Thus, according to the German design criterion, if the limit P/D of 1.5 could ensure the tightness of the UGS and SPR salt caverns, it means that the salt resources can be fully utilized and a number of existing abandoned salt caverns can be rebuilt for energy storage.

In this paper, a tightness analysis is presented of UGS and SPR salt caverns in bedded rock salt with a limit P/D of 1.5 in Jintan, China. The structure of this paper is as follows: In Section 2, the seepage mechanism in the surrounding rock is given, and the microcosmic, permeability and porosity tests are described. In Section 3, a 3D-geomechanical simulation model is built and the operating conditions are given. In Section 4, the numerical simulation results are obtained and the tightness evaluations of UGS and SPR salt caverns are conducted. In Section 5, some conclusions and proposals are put forward. The study provides a basic reference for constructing or rebuilding UGS/SPR facilities in bedded rock salt of Jintan, as well as a basic reference for similar engineering practices in other places.

II. SEEPAGE MECHANISM AND SEEPAGE PROPERTIES

A. SEEPAGE MECHANISM

The permeating flow media for the UGS salt cavern and the SPR salt cavern are gas and crude oil respectively. Generally, the flow of fluid in porous medium conforms to the Darcy theory [31], [32], which is expressed as

$$v = -\frac{k}{\mu}\nabla p \tag{1}$$

where k is the absolute permeability; ∇p means the pore pressure gradient; μ is the dynamic viscosity of the fluid.

The permeability test was carried out by the steady-state method. N^2 is used as the permeating flow medium during the permeability test. The permeability is generally calculated by the following function:

$$K_g = \frac{2P_0 Q_g \mu_g L}{A\left(P_{\text{in}}^2 - P_{\text{out}}^2\right)} \tag{2}$$

where K_g is the gas permeability, m^2; A is the cross-sectional area of the sample, m^2; L is the length of the mudstone sample, m; P_{in} and P_{out} are upstream absolute pressure and downstream absolute pressure respectively, Pa; μ_g is the dynamic viscosity of nitrogen, μPa·s; Q_g is gas flow, ml/s.

It is often found that the permeability measured by gas is much larger than that measured by liquid [33], [34]. This is mainly due to the difference of the seepage characteristics between gases and liquids. The flow velocity of the gas molecules will not be zero adjacent to the inner surface of a

TABLE 1. Results of the permeability and porosity tests.

NO.	K_g/md	K_∞/md	Φ(%)	K_g/md	K_∞/md	Φ(%)	K_∞/md	Φ(%)
1	0.074	0.057	6.83	0.622	0.504	13.85	—	1.33
2	0.105	0.088	7.39	0.616	0.467	11.38	—	0.93
3	0.066	0.052	7.72	0.544	0.423	11.87	—	1.61
4	0.098	0.081	8.44	0.538	0.416	14.32	—	1.02
5	0.087	0.062	7.82	0.605	0.440	12.73	—	0.71
Average	0.086	0.068	7.64	0.585	0.450	12.83	5e-4	1.12

seepage channel, and the liquids have a higher viscosity coefficient and greater interaction among molecules than gases and hence behave with an obvious boundary layer effect, which will result in the gas permeability is higher than the liquid permeability (absolute permeability) [26], [35]. When the salt caverns are used for UGS, K_a can be considered as its permeability during the natural gas seepage through the surrounding rock. When the salt caverns are for SPR, the intrinsic permeability should be used as its permeability. Due to the low permeability of the surrounding rock, the Klinkenberg effect should be considered during the permeability test. Klinkenberg showed experimentally that in low-permeability porous media the intrinsic permeability to gases is significantly higher than the permeability to liquids [36]. The Klinkenberg effect on gas permeability can be written as follows [37]–[39]

$$K_g = K_\infty \left(1 + \frac{b}{\overline{P}}\right) \approx K_\infty \left(1 + \frac{b}{P_{\text{in}} + P_{\text{out}}}\right) = K_\infty (1+f)\,,$$
$$f = \frac{b}{P_{\text{in}} + P_{\text{out}}} \tag{3}$$

where K_g is the gas permeability, m^2; K_∞ is the absolute permeability, m^2; P is the mean gas pressure, psi; b is the Klinkenberg coefficient, which depends on the pore structure of the porous medium and the mean free path of the given gas molecules, and generally decreases with increased permeability. The Klinkenberg coefficient is given by the equation [40]:

$$b = \frac{16c\mu_g}{\overline{w}}\sqrt{\frac{2RT}{\pi M}} \tag{4}$$

where c is a constant (typically taken as 0.9); μ_g is the dynamic viscosity of the gas, μPa·s; M is the molecular weight of gas; w is the mean pore diameter of the sample; R is the universal gas constant (8.3143 $J{\cdot}mol^{-1}{\cdot}K^{-1}$) and T is the absolute temperature. Considering the high viscosity of crude oil, the seepage of crude oil in the vicinity of the cavern must be very slow when the caverns are filled with oil compared to when gas is stored. Hydraulic conductivity is the parameter to demonstrate the seepage rate of a fluid in porous rock and is determined by

$$\kappa = K_\infty \rho g / \mu_{oil} \tag{5}$$

where k is the hydraulic parameter, m/s; ρ is the density of crude oil, kg/m^3; g is the gravitational acceleration, m/s^2; μ_{oil} is the dynamic viscosity coefficient of crude oil, mpa·s. Thus, the permeation rate of crude oil will be much lower than that of gas. In this paper, the density of the crude oil is 0.85×10^3 kg/m^3 and the dynamic viscosity coefficient of that is 9.012 MPa·s.

B. PERMEABILITY AND POROSITY OF THE SURROUNDING ROCK

High integrity and low permeability of surrounding rock are preconditions for energy storage. Although the permeability of salt is usually low, the excavation disturbed zone damage will more likely be generated quickly and many macroscopic fractures may even be generated in the interlayers and caprock. Thus, to study the seepage properties of the surrounding rock is necessary and that provides the basis for analyzing the tightness of the underground energy storage caverns. Cores of caprock and interlayers have been extracted from the target formation of Jintan salt mine range from 900 to 1000 m. Wire-cutting by KDXQ-II sample manufacture equipment was used to prepare the rock samples, which induced little damage to the rock and ensured the accuracy of less than 0.2 mm. Permeability and porosity tests were carried out on the KS-5 porosity-permeability measuring equipment designed by our research group to obtain the seepage properties of the caprock and interlayers. The process of wire cutting and the KS-5 porosity-permeability measuring equipment are shown in FIGURE 3. The parameters during the test processing are optimized by the hybrid algorithm to make the results more accurate [41]–[43]. The test results of gas permeability K_g, the absolute permeability $K\infty$ calculated by EQUATION (3) and the porosities are shown in TABLE 1. Due to the extremely low permeability of rock salt, the seepage property of rock salt cannot be measured by the steady-state method. In this paper, the permeability of rock salt is set as $5\times e^{-19}$ m^2 according to our previous research measured by the transient method [44]. According to the test results, the average permeabilities of interlayers and caprock are much higher than that of rock salt while the porosities are much lower than that of rock salt. This indicates that the seepage of gas and oil along the interlayers and caprock will be faster. The interlayers around the cavern will be the main flow channels because the gas and oil cannot easily breakthrough through the rock salt to the caprock. However, once the gas or oil seepage over the rock salt and break through the caprock, it will bring a great risk of leakage and contamination.

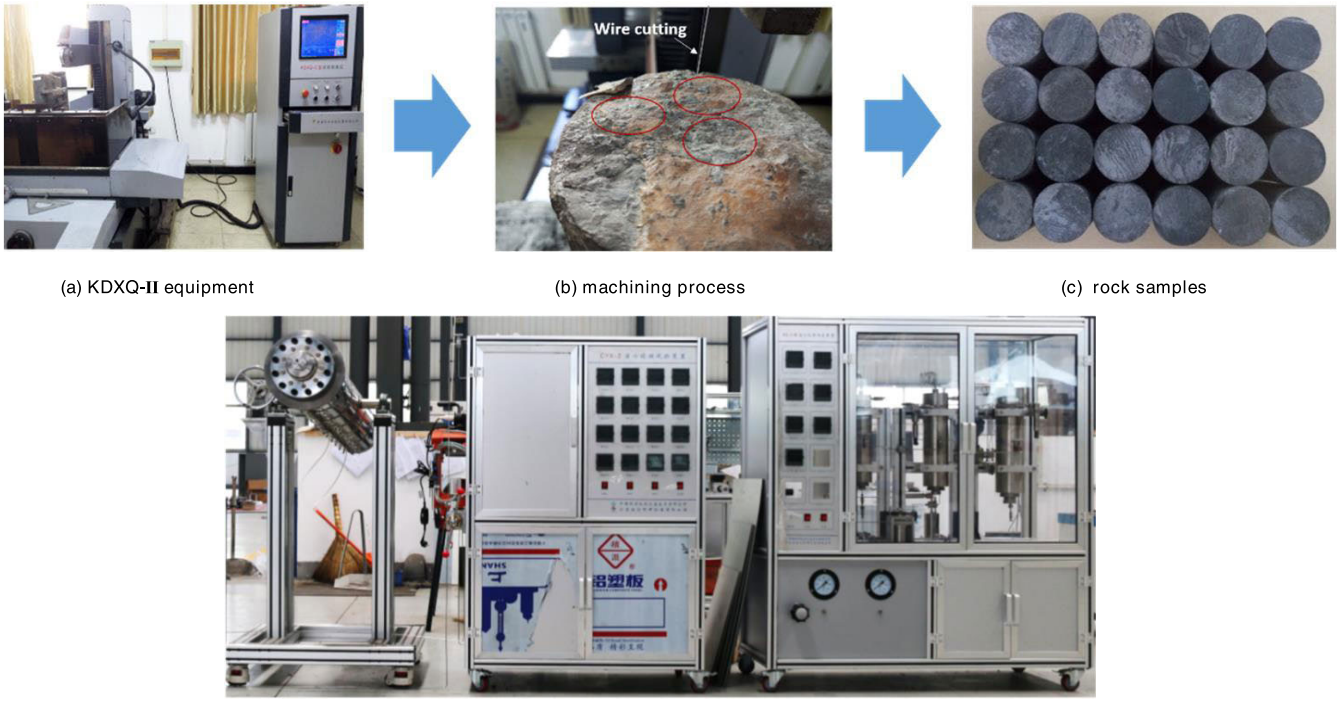

(a) KDXQ-II equipment (b) machining process (c) rock samples

(d) KS-5 porosity-permeability measuring equipment

FIGURE 3. Wire cutting and the KS-5 porosity-permeability measuring equipment.

The average values of the permeability and porosity are used for the later numerical simulations.

C. MICROSCOPIC PORE STRUCTURE OF THE SURROUNDING ROCK

Determining the microscopic pore structure of the surrounding rock of salt cavern is also a must for tightness analyzing and is helpful to explain the macro phenomenon during the permeability tests. The microstructure of the surrounding rock has been analyzed by scanning electron microscope (SEM). Considering that the surrounding rock is permeated by natural gas or crude oil, the SEM test conditions are divided into two groups: natural condition and crude oil immersion. The SEM samples of the crude oil immersion group are immersed in crude oil with a pressure of 15 MPa for 10 days and then are dried for 1 day at 100°C. The SEM results are shown in FIGURE 4. The images have been magnified 2000 times.

As is shown in FIGURE 4 (a), FIGURE 4 (c) and FIGURE 4 (e), the particle sizes of caprock and interlayers are much smaller and the particle spacing is obviously larger than that of rock salt. That is the reason why the permeability of caprock and interlayer are much lower than that of rock salt and the porosity of caprock and interlayer is much larger than rock salt. Comparing FIGURE 4 (a) and FIGURE 4 (b), the scanning plane of the caprock sample immersed by crude oil is obviously covered by some white thick substance. That is the asphaltene and resin of crude oil attached to the surface of the mineral particles and blocking their pore spaces. This observation also applies to FIGURE 4 (c) and FIGURE 4 (d), FIGURE 4 (e) and FIGURE 4 (f). This phenomenon indicates that the effect of oil immersion will have an influence on the seepage of the rock surrounding the salt cavern, especially for interlayers and caprock. We assumed that the permeability of the surrounding rock would be a bit lower after oil immersion. This is beneficial for the cavern tightness during the crude oil storage.

III. NUMERICAL SIMULATION AND OPERATING CONDITIONS

A. THE NUMERICAL MODEL

To analyze the seepage and leakage in the rock masses around the salt caverns, a 3D numerical model of two adjacent underground salt caverns is built based on the geological features of Jintan salt mine using the software ANSYS due to its powerful preprocess modeling function. This model has also been used for stability analysis and availability evaluation of the salt caverns of Jintan in our previous research [18]. Due to the small inclination angle of the strata according to the geological survey data [45], the strata in this numerical simulation are simplified to horizontal. To eliminate the boundary effect during the numerical simulation, a large enough axisymmetric model with dimensions of $800\times400\times800$ m in length, width and height respectively is built. Considering the model symmetry, the 1/2 model is shown in FIGURE 5. As is shown, the simulated depths range from 500 m to 1300 m. The target bedded rock salt formation has a thickness of nearly 200 m, wherein the energy storage salt caverns will

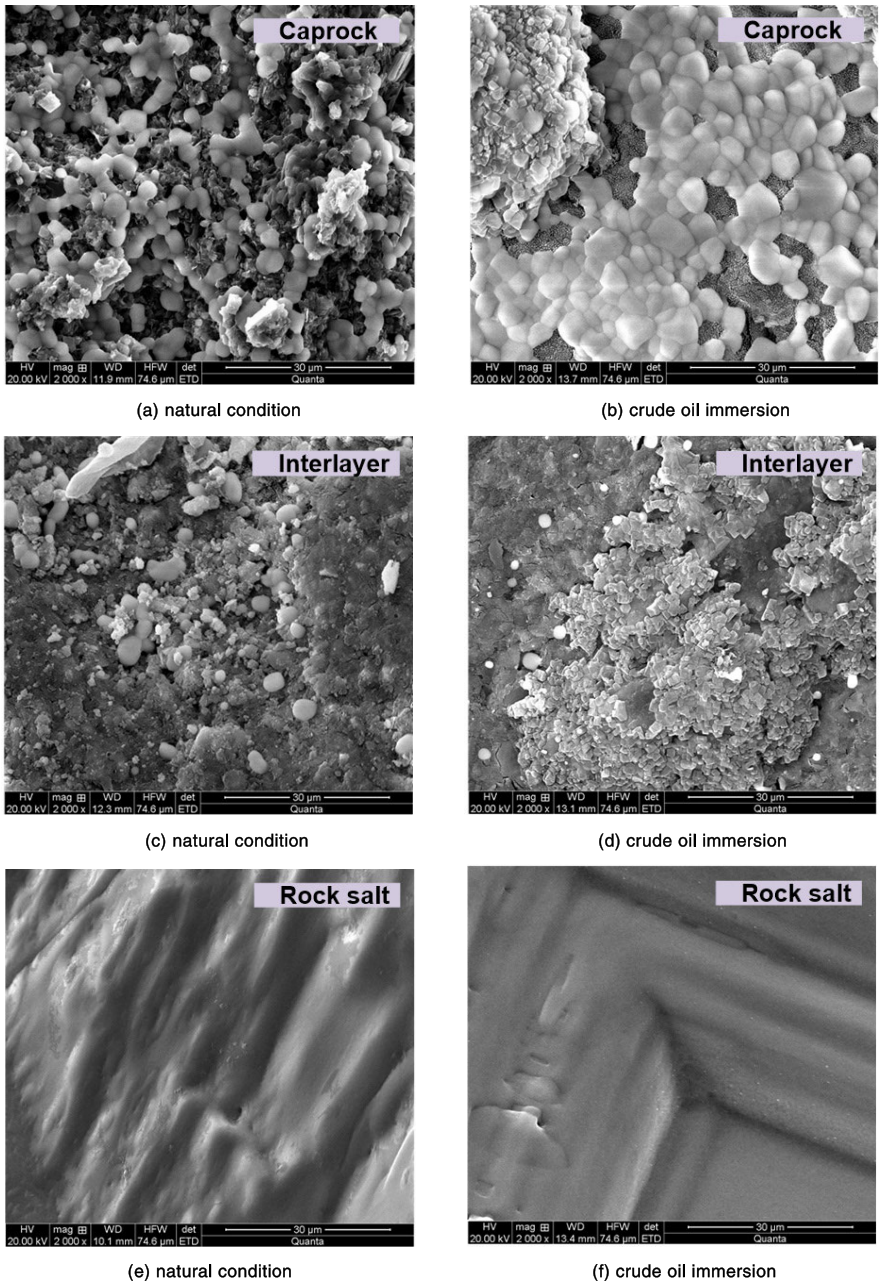

FIGURE 4. Scanning electron microscope (SAM) analysis of the surrounding rock.

be constructed. The depth ranges from 880 m to 1080 m. The cavern has a maximum diameter of 80 m and a total height of 130 m with a typical pear shape, i.e., the upper part is a half ellipsoid and the lower part is a half-sphere, based on previous engineering experiences. Both of the adjacent caverns are located in the middle of the numerical model, with a depth ranging from 930 m to 1060 m. Four interlayers with thicknesses of 1.25 m, 2.70 m, 2.35 m and 1.85 m respectively, are intersected by the salt caverns. The model is meshed by tetrahedron elements. It contains 111,420 nodes and 648,800 elements. To ensure the calculating accuracy and improve the numerical simulation efficiency, the element sizes are increased with increasing distance from the cavern. The mesh has been divided into 24 material blocks to model the individual material property. Among them, 10 material blocks shown in green represent salt formation, 4 material blocks shown in yellow represent the mudstone (caprock mudstone and floor rock mudstone), 8 material blocks shown in deep blue represent the interlayers and 2 material blocks in the middle set to null represent the caverns. After that, the model is introduced into FLAC^{3D} for the seepage calculation due to its powerful calculating capability in solving fluid

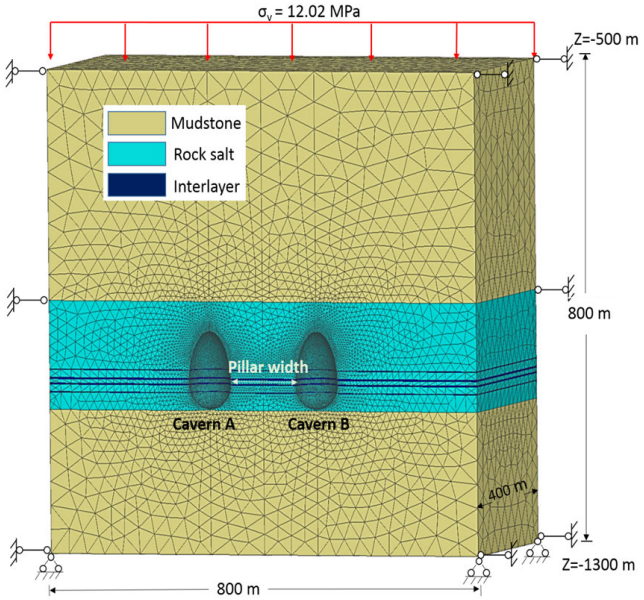

FIGURE 5. Numerical model and boundary conditions of energy storage salt caverns in bedding rock salt.

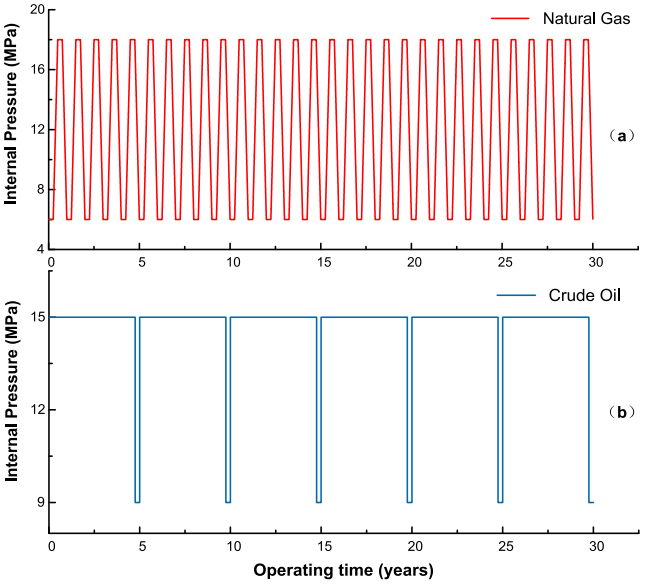

FIGURE 6. Cyclical internal pressure schematic diagram during the operating time for a UGS and an SPR cavern used in the numerical simulation.

seepage problems in geotechnical engineering. In FLAC^{3D} software, the boundary conditions of the numerical model are defined, shown in FIGURE 5. On the upper boundary, the axial stress of 12.02 MPa is applied, representing the overburden load (σ_v) at the top of the model calculated by the depth and the average gravity gradient of the overlying rock. The other five surfaces are set as the impermeable boundaries of the model and are all displacement constrained. Seepage parameters of the rock are defined based on the laboratory permeability and porosity tests result shown in TABLE 1. The initial geostress is given by $\sigma_H = \sigma_h = \sigma_v$ (σ_H and σ_h and the two principal horizontal stresses; σ_v is the vertical principal stress), because the geostress field in Jintan salt mine approximately approaches a hydrostatic state when the depth exceeds 432 m due to the excellent rheological property of rock salt in long-term deformation according to previous studies [46], [47]. The final numerical simulation results are post-processed by Tecplot [20].

B. CONDITIONS FOR TIGHTNESS ANALYSIS

The water solution mining method is used for the excavation of both the UGS and SPR salt caverns. According to available standards [48], [49], the design life of the underground energy storage salt caverns is at least 30 years, which is used in the calculations. During the operating time, synchronized injection-withdraw patterns are recommended because instability influence may occur in pillars if asynchronous injection-withdraw patterns are adopted [29].

As to the operating condition of UGS, because natural gas consumption changes significantly during different seasons, a one-year cycle in the UGS operating time can be divided into four stages. (1) Storage at minimum pressure; (2) Injection stage; (3) Storage at maximum pressure; (4) Production stage. The minimum and maximum internal gas pressures are about 6 MPa and 18 MPa respectively. The cyclical internal pressure schematic over the operating time of UGS is shown in FIGURE 6 (a).

The operating condition of an SPR is different from that of UGS. Because the purpose of an SPR is to protect national petroleum security and blunt the significant economic impacts of a shortage stemming from international events in times of crisis, the crude oil may stay in storage for decades. The internal pressure will be relatively constant for a long time. However, a workover phase is also needed to maintain the underground storage facilities operate. This process is designed to last for three months every 5 years. During this period, the wellhead pressure is dropped to 0 and the crude oil is at atmospheric pressure at ground level. The internal pressure of the SPR salt cavern can be calculated by the following equation:

$$P_{cavern} = P_{wellhead} + \rho_{oil} g h \tag{6}$$

where P_{cavern} is the internal pressure of the SPR salt cavern; $P_{wellhead}$ is the wellhead pressure applied on the surface; ρ_{oil} is the density of crude oil. g is the acceleration of gravity; h is the depth of crude oil. $P_{wellhead} = 6$ MPa is considered to be the optimum safety value according to the stability and availability evaluation of SPR salt caverns in Jintan [18]. The cyclical internal pressure schematic diagram during the operating time of an SPR is shown in FIGURE 6 (b).

The pillar to cavern diameter ratio (P/D) is an important measure used to establish a limit for the spacing between the caverns, where P is the pillar width and D is the maximum diameter of the salt cavern [28], [30]. Because the salt resources in Jintan are mainly bedded rock and the interlayers may be the main seepage channels, the tightness of the salt

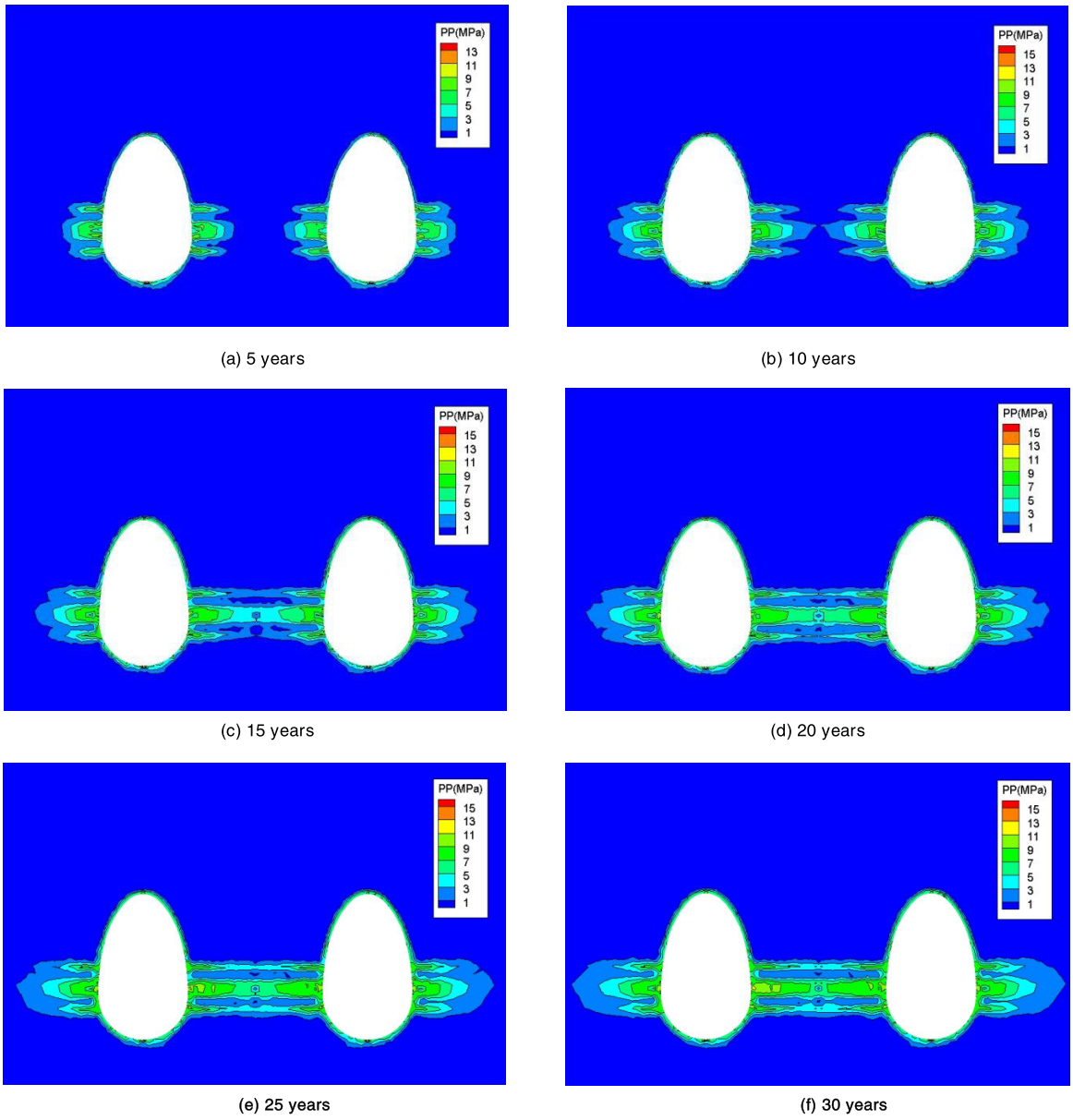

FIGURE 7. Seepage range, pore pressure (PP) contours around UGS caverns after different operating times.

cavern should be evaluated even though the cavern stability has been ensured. In this study, P/D is set as 1.5 to fully use the limited salt resources and ensure the stability of the caverns. Moreover, there are about thirty abandoned brine production caverns in Jintan salt mine and many of their P/D ratios are around 1.5. So, if the tightness of the UGS and SPR salt caverns could be ensured for a P/D of 1.5, it would mean that a number of existing abandoned salt caverns in Jintan salt mine could be rebuilt for energy storage. In this case, the salt resources in Jintan can be fully utilized and more salt caverns can be built for energy storage in this area.

Based on the previous studies of our research group, the conditions to assess the tightness of UGS salt cavern are presented as follows [26], [31]:

(1) The natural gas seepage should not break through into the caprock.

(2) The pore pressure in the middle of the pillar should be less than the minimum internal gas pressure.

(3) The total amount of natural gas leaked into the surrounding rock around the cavern should be less than 1%.

As for SPR salt caverns, when crude oil leaks into interlayers, the anhydrite in the mudstone interlayers will react with the naphthenic acid in the crude oil. The generated calcium naphthenate will dissolve in the crude oil. The reaction equation is expressed as

$$C_nH_{2n+1}COO^- + Ca^{2}+ \rightarrow (C_nH_{2n+1}COO)_2\,Ca \quad (7)$$

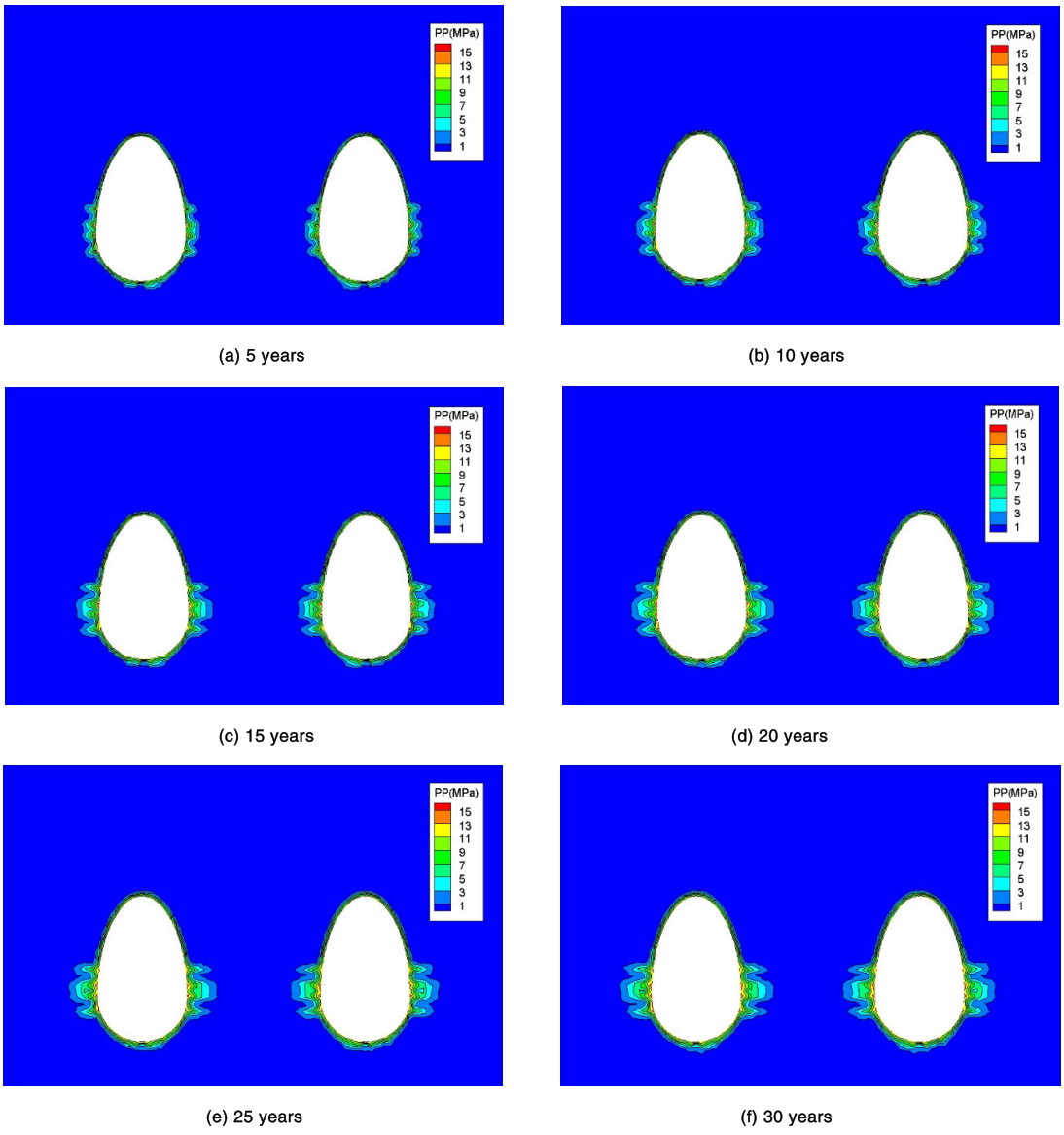

FIGURE 8. Seepage range, pore pressure (PP) contours around SPR caverns after different operating times.

The degree of reaction is related to the naphthenic acid content of crude oil. If the crude oil in the SPR salt cavern has a higher content of naphthenic acid, a large amount of chemical reaction may take place between the naphthenic acid and interlayers, which may influence the stability of the pillar.

Thus, considering the influence of the oil-rock interaction and combining the previous conditions, we propose the following conditions to assess the tightness of SPR salt caverns:

(1) The oil seepage should not break through into the caprock.

(2) To ensure the safety of the pillar, the seepage channels between the adjacent caverns should not connect to each other. (The pore pressure in the middle of the pillar should remain a constant value 0.)

(3) The total amount of crude oil leaked into the surrounding rock around the cavern should be less than 1%.

IV. ANALYSIS AND TIGHTNESS EVALUATION SEEPAGE

A. SEEPAGE AROUND THE UGS AND SPR SALT CAVERNS

From the numerical simulation results, the seepage range and seepage pore pressure around the UGS and SPR caverns are obtained, which are shown in FIGUREs 7 and 8 respectively. The results after operating 5, 10, 15, 20, 25, 30 years are listed to study the seepage evolution during the entire service life of the caverns. As is shown, the seepage pore pressures and the influence areas in the rock masses around the UGS and SPR caverns both increase with operating time. However, due to the low permeability and porosity of rock salt, the seepage velocity of natural gas and crude oil are both quite low and

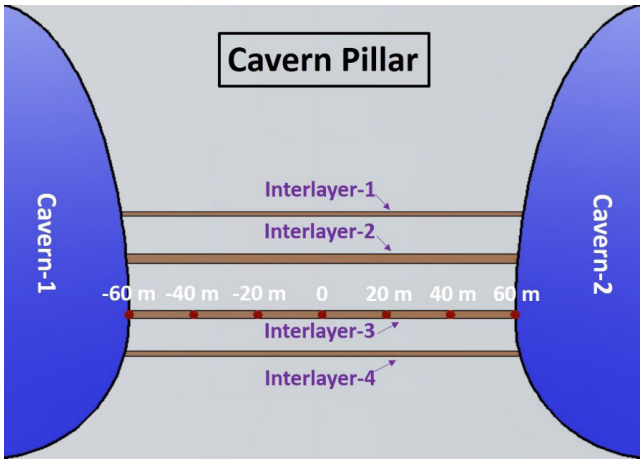

FIGURE 9. Locations of interlayers between the adjacent salt caverns.

the seepage cannot break through into the caprock according to the numerical simulation results. Both the UGS and SPR salt caverns under the current geological conditions can meet the tightness assessment criterion (1).

The seepage pressures and the penetration distances in the interlayers are much larger than those in the rock salt. This Indicates that the interlayers serve as the main channels for the natural gas or crude oil to seep through, which is consistent with the results of permeability and porosity tests. Thus, the interlayer is one of the key factors affecting cavern sealing. Therefore, the study on the gas/oil seepage in the interlayer should be the focus during the design of UGS/SPR salt cavern in bedded rock salt to eliminate its negative effects on the cavern and pillar safety.

The seepage pressure in the pillar between the adjacent salt caverns increases with time. As to the UGS caverns, if the zone with high gas pressure penetrates the entire pillar, it is disadvantageous for the pillar stability, especially when the internal pressure of the caverns changes cyclically. Comparing FIGUREs 7 and 8, it can be seen that the seepage velocity of natural gas in the interlayers around the UGS caverns is much faster than that of crude oil in the interlayers around the SPR caverns. After operating for 15 years, as shown in FIGURE 7 (c), the seepage areas of the UGS salt caverns in the interlayers begin to join together, and the pore pressure in the middle of the pillar becomes higher with time increasing. But the seepage areas of the SPR salt caverns in the interlayers after operating 15 years change slowly by comparing FIGURE 8 (b) and FIGURE 8 (c). That is due to the crude oil having a much higher viscosity coefficient and greater interaction among molecules, behaving with an obvious boundary layer effect. This property will be beneficial for the SPR salt caverns to be constructed under adverse geological conditions. It means that if the geological conditions are not so good, the salt caverns should preferably be used to store crude oil rather than natural gas so as to reduce the leakage risk.

B. PORE PRESSURE VARIATION ALONG THE INTERLAYER

Because the seepage in the interlayers has a significant influence on the tightness and safety of the pillar, thoroughly investigating the seepage evolution in the interlayers during the operating time of the UGS and SPR salt caverns is necessary. The locations of the interlayers are shown in FIGURE 9.

The relationships between gas seepage pressures in the interlayers and the distances to the middle of the pillar after UGS caverns operating for 30 years are shown in FIGURE 10. The relationships between oil seepage pressures in the interlayers and the distances to the middle of the pillar after SPR caverns operating for 30 years are shown in FIGURE 11. As is shown, due to the synchronous injection-withdraw patterns, the curves show symmetrical distribution along the middle of the pillar. The pore pressure distribution along each interlayer is not linear. After operating 29.75 years, the internal pressure reaches the maximum value and the distribution of the pore pressure along the interlayer shows a nonlinear decrease. However, after operating 30 years, when the internal pressure in the salt caverns turns to the minimum operating pressure, the pore pressure near the edge of the cavern also rapidly decreases to the minimum value. (Considering that the internal pressure changes periodically, the seepage pressure at the cavern edge will also change periodically.) But the pore pressure near the middle of the pillar almost remains constant. This indicates that the periodic variation of the internal pressure in a cavern has a great effect on the pore pressure around the cavern edge and the influence of that decreases gradually with the increase of seepage distance.

When the salt caverns are used for UGS, results show that the variation of pore pressure in each interlayer is different. The curves of interlayer-1 and interlayer-4 are nearly the same. Both of them are slightly smaller than the results of interlayer-2 and interlayer-3. This indicates that the position of the interlayer has an influence on the extent of gas leakage. The pore pressure along the interlayer becomes higher with a location closer to the waist of the cavern. Comparing the pore pressure in the middle of the pillar, it can be seen that the values in interlayer-1 and interlayer-4 are nearly 5 MPa. While the values in interlayer-2 and interlayer-3 are more than 7 MPa. According to the tightness assessment criterion (2) of UGS, the pore pressure in the middle of the pillar should be less than the minimum internal gas pressure (6 MPa). Therefore, based on the calculation results, the pore pressures in the middle of the pillar of interlayer-2 and interlayer-3 are above the threshold value of tightness assessment criterion (2). It means that the salt cavern group with a 1.5D pillar width cannot satisfy the tightness condition of UGS.

When the cavern is storing crude oil, the pore pressures along the interlayers decrease to 0 MPa once the seepage distance reaches around 13 m after the SPR cavern has operated for 30 years. It also means that the maximum seepage radiuses in the interlayers are about 13 m, much lower than for gas storage. According to the tightness assessment criterion (2)

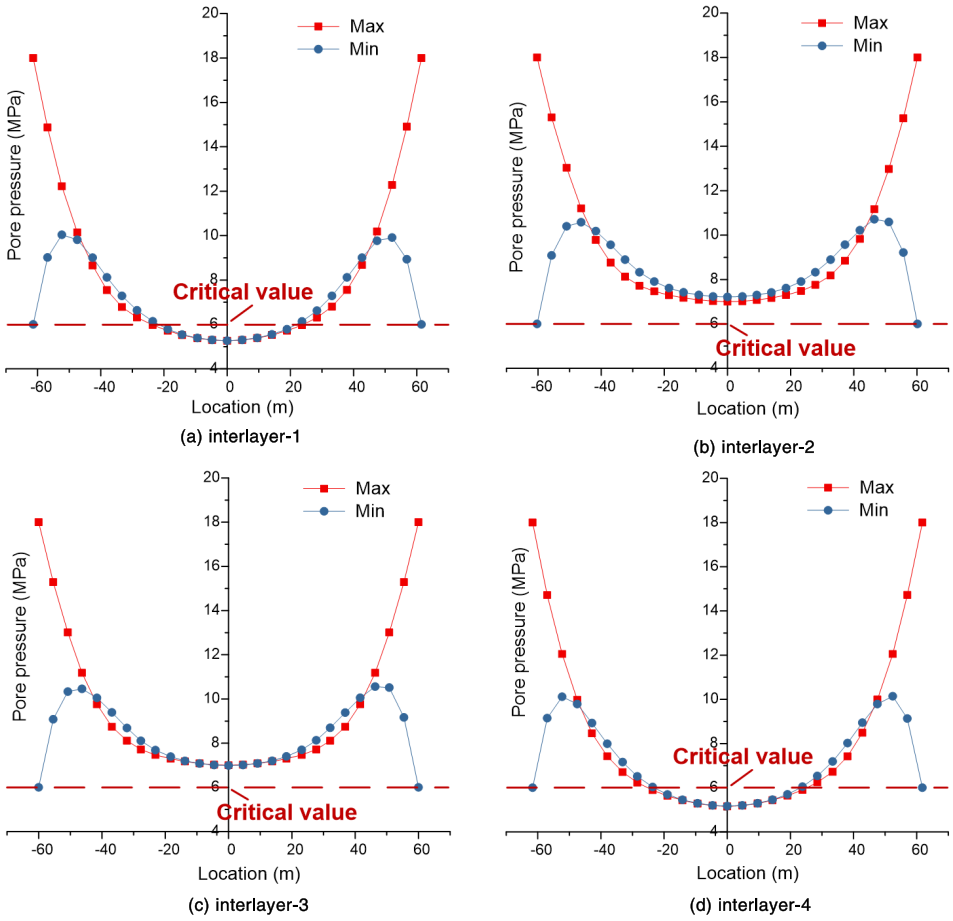

FIGURE 10. The relationships between gas seepage pressures in the interlayers and the distances to the middle of the pillar after UGS caverns have operated for 30 years. "Max." means the pore pressure along the interlayer when the maximum internal pressure (18 MPa) acted in the caverns over 29.75 years, "Min." means the pore pressure along the interlayer when the minimum internal pressure (6 MPa) was present in the caverns over 30 years.

of SPR, we consider that the salt cavern group with a 1.5D pillar width can satisfy this criterion because the crude oil leakage cannot penetrate through the pillar.

On the basis of the analysis above, it can be concluded that the caverns with a 1.5D pillar width are unsuitable to store natural gas. To ensure the safety of the salt caverns, designing or reconstructing these caverns for SPR is more preferable.

C. LOSS RATE OF THE LEAKAGE

FIGURE 12 presents the gas leakage range around interlayer-1, interlayer-2 interlayer-3, and interlayer-4 respectively after UGS salt caverns have operated for 30 years. FIGURE 13 presents the oil leakage range around interlayer-1, interlayer-2 interlayer-3, and interlayer-4 respectively after SPR salt caverns have operated for 30 years. For simplification, we just consider the leakage along with the interlayers, because the permeability of rock salt is extremely low. We consider the distance from the cavern edge to the point with a pore pressure of 0 MPa as the maximum seepage distance. As is shown, during the UGS operating time, the maximum seepage distances in these four interlayers are 83.64 m, 103.68 m, 98.90 m, 83.38 m, respectively. While during the SPR operating time, the maximum seepage distances along these four interlayers are just 12.99 m, 13.19 m, 13.31 m, 12.76 m. The results indicate that the seepage range in the interlayer of the natural gas storage caverns is much larger than that of crude oil storage caverns. However, this does not mean that the loss rate of natural gas is higher than that of crude oil because the calculation methods of the loss rates of natural gas and of oil are different. The amount of gas leakage is related to the pore pressure at each point along with the interlayers. For the crude oil storage period, the variations of the pore pressure along the interlayers are not related to the leakage amount due to the incompressibility of crude oil.

In this paper, we assume that the seepage range approximately satisfies the two-dimensional axisymmetric flow model regardless of whether the caverns are storing natural gas or crude oil, as is shown in FIGURE 14. The loss rate of these two-flow media can be calculated as follows.

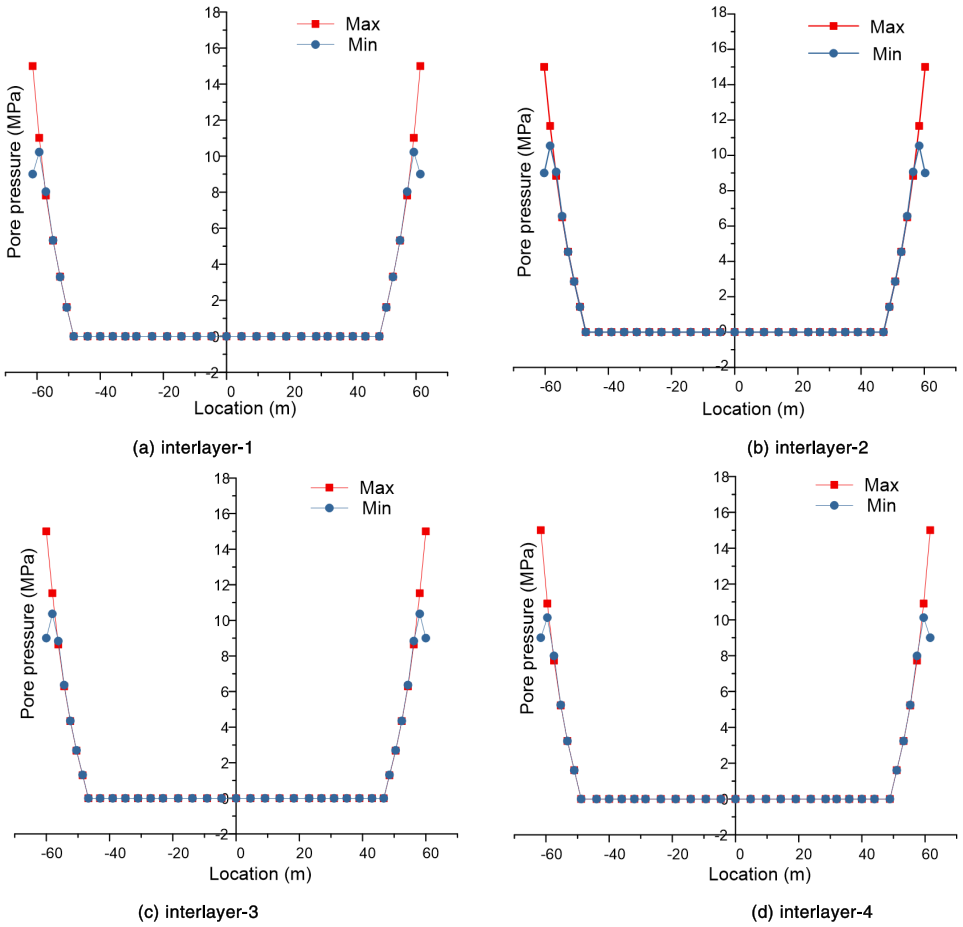

FIGURE 11. The relationships between oil seepage pressures in the interlayers and the distances to the middle of the pillar after SPR caverns have operated for 30 years. "Max." means the pore pressure along the interlayer when the maximum internal pressure (15 MPa) acted in the caverns over 29.75 years, "Min." means the pore pressure along the interlayer when the minimum internal pressure (0 MPa) was present in the caverns over 30 years.

For natural gas storage, based on the state equation of ideal gas:

$$P_0 V_{\text{cavern}} = P_{\text{air}} V_{\text{total}} \tag{8}$$

where P_0 is the internal pressure of the salt cavern at the moment; V_{cavern} is the total volume of a single cavern, nearly 33.4×10^4 m^3; P_{air} is the atmospheric pressure; V_{total} is the total storage volume of natural gas at atmospheric pressure. According to EQUATION (8), the calculation result of V_{total} is about 1.984×10^7 m^3.

$$\sum P_{\text{pore}} V_{\text{pore}} = P_{\text{air}} V_{\text{leakage}} \tag{9}$$

$$V^i_{leakage} = \int_0^{L_{\max}} 2\pi\,(R_i + s)\, h_i \varphi P_S / P_{air}\, ds \tag{10}$$

$$V_{leakage} = \frac{\sum_{i=1}^{4} \int_0^{L_{\max}} 2\pi\,(R_i + s)\, h_i \varphi P_S / P_{air}\, ds}{P_{air}} \tag{11}$$

where P_{pore} is the pore pressure at any point along the interlayer; V_{pore} is the pore volume at any point along the interlayer; V_{leakage} is the leakage amount of natural gas of interlayer-i at atmospheric pressure; V_{leakage} is the total leakage amount of natural gas at atmospheric pressure; $L_{\max}$ is the maximum seepage distance; R_i is the radius of the cross-section of the cavern at the location of interlayer-i (These four radii are 38.7 m, 39.81 m, 40.00 m and 38.24 m respectively); S is the distance from the current point to the cavern edge; h_i is the thickness of interlayer-i; φ is the porosity of the interlayers; P_s is the pore pressure at the current point.

According to the analysis results presented in FIGURE 12, and based on EQUATION (10), the leakage amounts of natural gas of interlayer-1, interlayer-2, interlayer-3, and interlayer-4 are 149773 m^3, 396457 m^3, 329207 m^3 and 202372 m^3, respectively. The value of V_{leakage} is 1077809 m^3.

Thus, the loss rate of the leakage during the natural gas storage period can be calculated as

$$\Phi^{\text{gas}}_{\text{leakage}} = \frac{V_{\text{leakage}}}{V_{\text{total}}} \times 100\% = 5.43\% \tag{12}$$

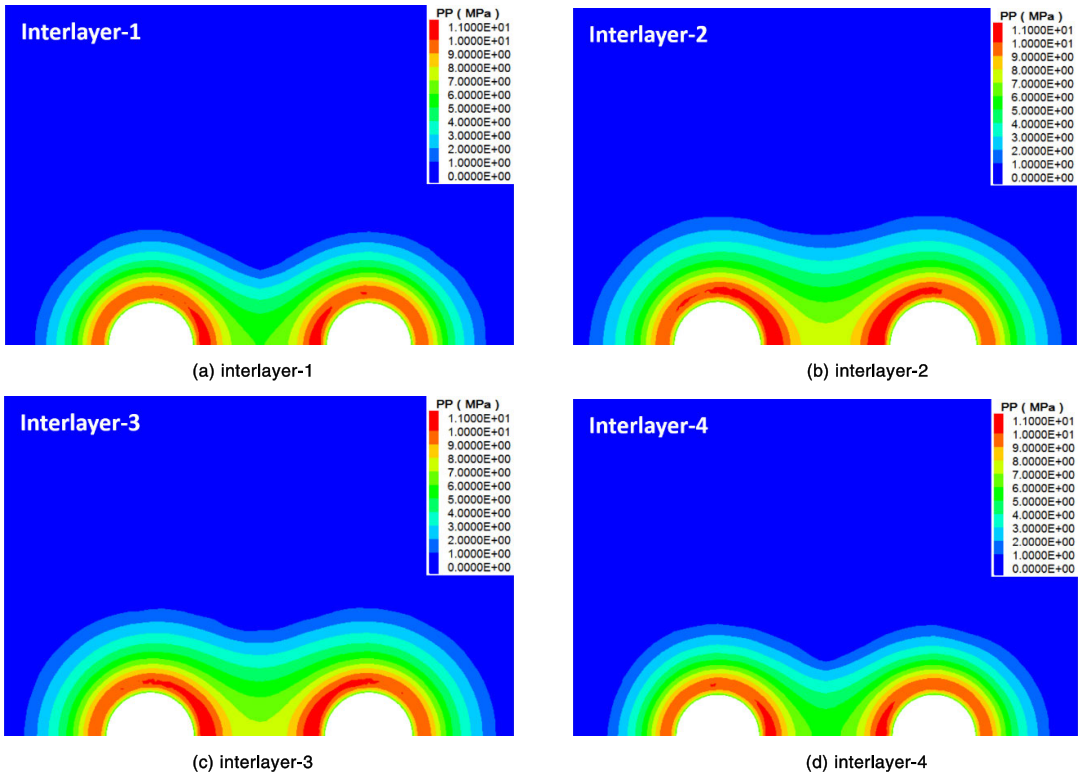

FIGURE 12. Gas seepage range around different interlayers after operating for 30 years.

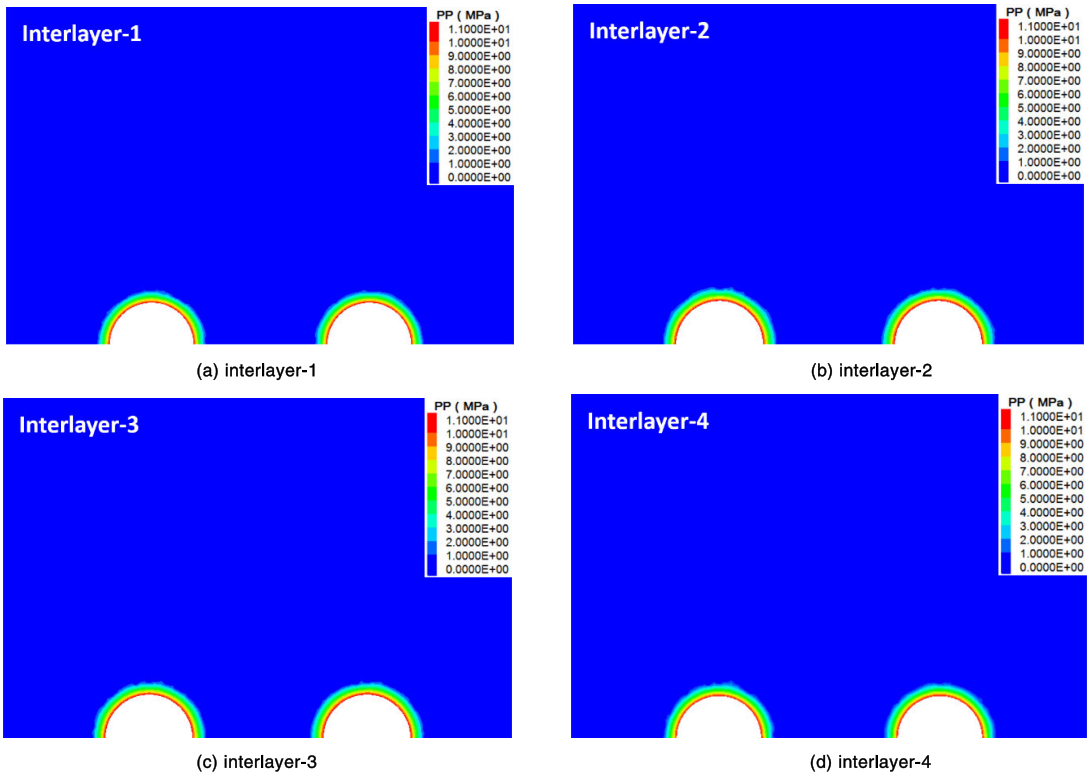

FIGURE 13. Oil seepage range around different interlayers after operating for 30 years.

All the factors such as the porosity of the interlayers, the thickness of the interlayers, the number of interlayers and the internal pressure in salt caverns have a great influence on the leakage of natural gas. Under the current conditions, the loss rate of the leakage of natural gas has exceeded the threshold value (1%) according to the tightness assessment

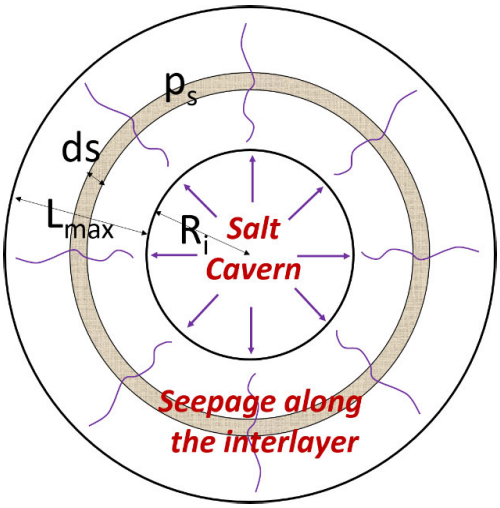

FIGURE 14. Model of two-dimensional axisymmetric flow.

criterion (3) of UGS. It means that the geological conditions around the salt caverns cannot satisfy the tightness requirement of UGS.

As to the SPR salt caverns, the leakage of crude oil can be calculated by EQUATION (13) due to its incompressibility. The total storage amount of crude oil equals the volume of salt caverns.

$$V_{leakage} = \int_0^{L_{max}} 2\pi\,(R_i + s)\,h_i \varphi ds \tag{13}$$

According to the analysis results in FIGURE 13, the leakage volumes of crude oil of interlayer-1, interlayer-2, interlayer-3, and interlayer-4 are 378.08 m^3, 851.10 m^3, 751.54 m^3, and 542.45 m^3, respectively. V_{leakage} is 2523.17 m^3.

Thus, the loss rate of the leakage can be calculated as

$$\Phi^{\text{oil}}_{\text{leakage}} = \frac{V_{\text{leakage}}}{V_{\text{total}}} \times 100\% = 0.76\% \tag{14}$$

According to the tightness assessment criterion (3) of SPR, the loss rate of the leakage is less than 1%, which satisfies the tightness requirement.

The loss rate of the SPR is much lower than that of the UGS and the loss rate of the UGS cannot meet the tightness assessment criterion (3). It can be concluded that to minimize the energy loss using these salt caverns for SPR is preferable rather than for UGS.

V. CONCLUSION

This paper aims to study the tightness of underground gas storage (UGS) and strategic petroleum reserve (SPR) caverns in bedded rock salt with limit pillar widths of Jintan, Jiangsu province, China. Pillar widths are one controlling limit on cavern design. Permeability and porosity tests have been carried out to determine the basic data for the tightness assessment. Microscopic characterization of the surrounding rock is given. The operational conditions and the numerical simulation results of UGS and SPR salt caverns have been discussed. The main conclusions and proposals are as follows:

(1) The permeability and porosity test results show that the average permeability of interlayers and caprock are much higher than that of rock salt while the porosities are much lower than that of rock salt. This indicates that the seepage of gas and oil along the interlayers and caprock will be faster than through rock salt. The interlayers around the cavern will be the main flow channels during energy storage because gas and oil cannot easily break through the rock salt to the caprock. However, it may bring a great risk of leakage and contamination once the gas or oil breakthrough the caprock.

(2) According to the microanalysis result of surrounding rock, it can be concluded that oil immersion influences the seepage of the rock surrounding salt caverns. It causes its permeability to be even lower due to the asphaltene and resin contents of crude oil attaching to the surface of the mineral particles of the rock and blocking their pore spaces. This is beneficial for the cavern tightness during crude oil storage.

(3) According to the numerical simulation results, the seepage velocity, the seepage range and the fluid loss rate of the SPR salt caverns are much lower than those of UGS salt caverns. This indicates that if the geological conditions are not so good, the salt caverns should preferably be used to store crude oil rather than natural gas so as to reduce the leakage risk.

(4) A limit pillar width with a pillar to diameter ratio (P/D) of 1.5 is confirmed to satisfy the tightness of SPR salt caverns, while it cannot meet the requirement of UGS. This means that the existing abandoned salt caverns in Jintan with P/D of around 1.5 which are unsuitable for UGS have the potential to be rebuilt for SPR. This would significantly increase the crude oil storage capacity of China.

Although some important and interesting conclusions have been obtained in this study, there is still some shortcomings. For example, the parameters in the model are fixed, and some meta-heuristic algorithms [50], [51] are needed to optimize the parameters to obtain more accurate simulation results.

REFERENCES

[1] W. Qiao and H. Wang, "Analysis of the wellhead growth in HPHT gas wells considering the multiple annuli pressure during production," *J. Natural Gas Sci. Eng.*, vol. 50, pp. 43–54, Feb. 2018.

[2] W. Qiao, Z. Yang, Z. Kang, and Z. Pan, "Short-term natural gas consumption prediction based on Volterra adaptive filter and improved whale optimization algorithm," *Eng. Appl. Artif. Intell.*, vol. 87, Jan. 2020, Art. no. 103323.

[3] W. Qiao, K. Huang, M. Azimi, and S. Han, "A novel hybrid prediction model for hourly gas consumption in supply side based on improved whale optimization algorithm and relevance vector machine," *IEEE Access*, vol. 7, pp. 88218–88230, 2019.

[4] C. Zhao and B. Chen, "China's oil security from the supply chain perspective: A review," *Appl. Energy*, vol. 136, pp. 269–279, Dec. 2014.

[5] J. Chen, W. Liu, D. Jiang, J. Zhang, S. Ren, L. Li, X. Li, and X. Shi, "Preliminary investigation on the feasibility of a clean CAES system coupled with wind and solar energy in China," *Energy*, vol. 127, pp. 462–478, May 2017.

[6] W. Qiao, W. Tian, Y. Tian, Q. Yang, Y. Wang, and J. Zhang, "The forecasting of PM2.5 using a hybrid model based on wavelet transform and an improved deep learning algorithm," *IEEE Access*, vol. 7, pp. 142814–142825, 2019.

[7] [Online]. Available: http://www.boaoforum.org/
[8] G. Wu, Y.-M. Wei, C. Nielsen, X. Lu, and M. B. Mcelroy, "A dynamic programming model of China's strategic petroleum reserve: General strategy and the effect of emergencies," *Energy Econ.*, vol. 34, no. 4, pp. 1234–1243, Jul. 2012.
[9] C. De Jong, "Gas storage valuation and optimization," *J. Natural Gas Sci. Eng.*, vol. 24, pp. 365–378, May 2015.
[10] J. Fan, D. Jiang, W. Liu, F. Wu, J. Chen, and J. Daemen, "Discontinuous fatigue of salt rock with low-stress intervals," *Int. J. Rock Mech. Mining Sci.*, vol. 115, pp. 77–86, Mar. 2019.
[11] L. Jinlong, X. Wenjie, Z. Jianjing, L. Wei, S. Xilin, and Y. Chunhe, "Modeling the mining of energy storage salt caverns using a structural dynamic mesh," *Energy*, vol. 193, Feb. 2020, Art. no. 116730.
[12] W. Liu, Z. Zhang, J. Chen, J. Fan, D. Jiang, D. Jjk, and Y. Li, "Physical simulation of construction and control of two butted-well horizontal cavern energy storage using large molded rock salt specimens," *Energy*, vol. 185, pp. 682–694, Oct. 2019.
[13] T. Wang, C. Yang, H. Wang, S. Ding, and J. Daemen, "Debrining prediction of a salt cavern used for compressed air energy storage," *Energy*, vol. 147, pp. 464–476, Mar. 2018.
[14] J. Li, Y. Tang, X. Shi, W. Xu, and C. Yang, "Modeling the construction of energy storage salt caverns in bedded salt," *Appl. Energy*, vol. 255, Dec. 2019, Art. no. 113866.
[15] W. Liu, X. Zhang, J. Fan, Y. Li, and L. Wang, "Potential evaluation of salt cavern gas storage in the Yangtze River Delta region and integration of brine extraction-cavern utilization," *Natural Resour. Res.*, to be published.
[16] J. Chen, D. Lu, W. Liu, J. Fan, D. Jiang, L. Yi, and Y. Kang, "Stability study and optimization design of small-spacing two-well (SSTW) salt caverns for natural gas storages," *J. Energy Storage*, vol. 27, Feb. 2020, Art. no. 101131.
[17] X. Shi, W. Liu, J. Chen, C. Yang, Y. Li, H. Ma, H. Peng, T. Wang, and X. Ma, "Geological feasibility of underground oil storage in Jintan salt mine of China," *Adv. Mater. Sci. Eng.*, vol. 2017, pp. 1–11, 2017.
[18] N. Zhang, X. Shi, T. Wang, C. Yang, W. Liu, H. Ma, and J. Daemen, "Stability and availability evaluation of underground strategic petroleum reserve (SPR) caverns in bedded rock salt of Jintan, China," *Energy*, vol. 134, pp. 504–514, Sep. 2017.
[19] T. Wang, S. Ding, H. Wang, C. Yang, X. Shi, H. Ma, and J. Daemen, "Mathematic modelling of the debrining for a salt cavern gas storage," *J. Natural Gas Sci. Eng.*, vol. 50, pp. 205–214, Feb. 2018.
[20] T. Wang, C. Yang, J. Chen, and J. Daemen, "Geomechanical investigation of roof failure of China's first gas storage salt cavern," *Eng. Geol.*, vol. 243, pp. 59–69, Sep. 2018.
[21] T. Wang, H. Ma, X. Shi, C. Yang, N. Zhang, J. Li, S. Ding, and J. Daemen, "Salt cavern gas storage in an ultra-deep formation in Hubei, China," *Int. J. Rock Mech. Mining Sci.*, vol. 102, pp. 57–70, Feb. 2018.
[22] W. Liang, C. Yang, Y. Zhao, M. Dusseault, and J. Liu, "Experimental investigation of mechanical properties of bedded salt rock," *Int. J. Rock Mech. Mining Sci.*, vol. 44, no. 3, pp. 400–411, Apr. 2007.
[23] Z. Hou, "Mechanical and hydraulic behavior of rock salt in the excavation disturbed zone around underground facilities," *Int. J. Rock Mech. Mining Sci.*, vol. 40, no. 5, pp. 725–738, Jul. 2003.
[24] Z. Deng and S. Wang, "Breaking pressure of gas cap rocks," (in Chinese), *Oil Gas Geol.*, vol. 21, no. 2, pp. 136–138, 2000.
[25] K. Staudtmeister and R. Rokahr, "Rock mechanical design of storage caverns for natural gas in rock salt mass," *Int. J. Rock Mech. Mining Sci.*, vol. 34, nos. 3–4, pp. 300.e1–300.e13, Apr. 1997.
[26] L. Wei, C. Jie, J. Deyi, S. Xilin, L. Yinping, J. Daemen, and Y. Chunhe, "Tightness and suitability evaluation of abandoned salt caverns served as hydrocarbon energies storage under adverse geological conditions (AGC)," *Appl. Energy*, vol. 178, pp. 703–720, Sep. 2016.
[27] K. Khaledi, E. Mahmoudi, M. Datcheva, and T. Schanz, "Stability and serviceability of underground energy storage caverns in rock salt subjected to mechanical cyclic loading," *Int. J. Rock Mech. Mining Sci.*, vol. 86, pp. 115–131, Jul. 2016.
[28] L. L. Van Sambeek, "Salt pillar design equation," in *Science of Rock Mechanics* (Series on Rock & Soil Mechanics). 1998.
[29] T. Wang, C. Yang, X. Yan, and J. Daemen, "Allowable pillar width for bedded rock salt caverns gas storage," *J. Petroleum Sci. Eng.*, vol. 127, pp. 433–444, Mar. 2015.
[30] B. L. Ehgartner and B. Y. Park, "Allowable pillar to diameter ratio for strategic petroleum reserve caverns," Office Sci. Tech. Inf., Tech. Rep., 2011.
[31] T. Wang, H. Ma, C. Yang, X. Shi, and J. Daemen, "Gas seepage around bedded salt cavern gas storage," *J. Natural Gas Sci. Eng.*, vol. 26, pp. 61–71, Sep. 2015.
[32] J. Fan, H. Xie, J. Chen, D. Jiang, C. Li, W. Ngaha Tiedeu, and J. Ambre, "Preliminary feasibility analysis of a hybrid pumped-hydro energy storage system using abandoned coal mine goafs," *Appl. Energy*, vol. 258, Jan. 2020, Art. no. 114007, doi: 10.1016/j.apenergy.2019.114007.
[33] P. F. Shan and X. P. Lai, "Numerical simulation of the fluid-solid coupling process during the failure of a fractured coal-rock mass based on the regional geostress," *Transp. Porous Med.*, vol. 124, no. 3, pp. 1061–1079, Sep. 2018.
[34] P. Shan and X. Lai, "Influence of CT scanning parameters on rock and soil images," *J. Vis. Commun. Image Represent.*, vol. 58, pp. 642–650, Jan. 2019.
[35] W. Liu, N. Muhammad, J. Chen, C. Spiers, C. Peach, J. Deyi, and Y. Li, "Investigation on the permeability characteristics of bedded salt rocks and the tightness of natural gas caverns in such formations," *J. Natural Gas Sci. Eng.*, vol. 35, pp. 468–482, Sep. 2016.
[36] P. Cosenza, M. Ghoreychi, B. Bazargan-Sabet, and G. De Marsily, "*In situ* rock salt permeability measurement for long term safety assessment of storage," *Int. J. Rock Mech. Mining Sci.*, vol. 36, no. 4, pp. 509–526, Jun. 1999.
[37] J. J. Kaluarachchi, "Analytical solution to two-dimensional axisymmetric gas flow with klinkenberg effect," *J. Environ. Eng.*, vol. 121, no. 5, pp. 417–420, May 1995.
[38] Q. Liu, Y. Cheng, H. Zhou, P. Guo, F. An, and H. Chen, "A mathematical model of coupled gas flow and coal deformation with gas diffusion and klinkenberg effects," *Rock Mech. Rock Eng.*, vol. 48, no. 3, pp. 1163–1180, May 2015.
[39] G. Wang, T. Ren, K. Wang, and A. Zhou, "Improved apparent permeability models of gas flow in coal with Klinkenberg effect," *Fuel*, vol. 128, pp. 53–61, Jul. 2014.
[40] Z. Zhang, D. Jiang, W. Liu, J. Chen, E. Li, and J. Fan, "Study on the mechanism of roof collapse and leakage of horizontal cavern in thinly bedded salt rocks," *Environ. Earth Sci.*, vol. 78, no. 10, p. 292, 2019.
[41] W. Qiao, H. Lu, G. Zhou, M. Azimi, Q. Yang, and W. Tian, "A hybrid algorithm for carbon dioxide emissions forecasting based on improved lion swarm optimizer," *J. Cleaner Prod.*, vol. 244, Jan. 2020, Art. no. 118612.
[42] W. Qiao and Z. Yang, "An improved dolphin swarm algorithm based on kernel fuzzy C-means in the application of solving the optimal problems of large-scale function," *IEEE Access*, vol. 8, pp. 2073–2089, 2020, doi: 10.1109/access.2019.2958456.
[43] W. Qiao and Z. Yang, "Forecast the electricity price of U.S. using a wavelet transform-based hybrid model," *Energy*, vol. 193, Feb. 2020, Art. no. 116704, doi: 10.1016/j.energy.2019.116704.
[44] S. Chen, C. Yang, and G. Wang, "Evolution of thermal damage and permeability of Beishan granite," *Appl. Therm. Eng.*, vol. 110, pp. 1533–1542, Jan. 2017.
[45] C. Yang, T. Wang, Y. Li, H. Yang, J. Li, D. Qu, B. Xu, Y. Yang, and J. Daemen, "Feasibility analysis of using abandoned salt caverns for large-scale underground energy storage in China," *Appl. Energy*, vol. 137, pp. 467–481, Jan. 2015.
[46] L. Ma, X. Liu, S. Ma, and D. Wang, "Numerical analysis of *in-situ* ground stress in deeprock salt stratum containing mudstone inter-layers," (in Chinese), *J. Univ. Sci. Technol. (Natural Sci. Ed.)*, vol. 10, pp. 604–609, 2009.
[47] D. Zhao, Z. Chen, X. Cai, and S. Li, "Analysis of distribution rule of geostress in China," (in Chinese), *Chin. J. Rock Mech. Eng.*, vol. 26, pp. 1265–1271, 2007.
[48] C. Feng, L. Zhaoyuan, C. Jianqiang, C. Bo, Y. Yanbin, L. Changlu, and J. Chong, "Research on reducing mining-induced disasters by filling in steeply inclined thick coal seams," *Sustainability*, vol. 11, no. 20, p. 5802, Oct. 2019.
[49] F. Cui, Y. Yang, X. Lai, C. Jia, and P. Shan, "Experimental study on the effect of advancing speed and stoping time on the energy release of overburden in an upward mining coal working face with a hard roof," *Sustainability*, vol. 12, no. 1, p. 37, Dec. 2019.
[50] W. Qiao and Z. Yang, "Modified dolphin swarm algorithm based on chaotic maps for solving high-dimensional function optimization problems," *IEEE Access*, vol. 7, pp. 110472–110486, 2019.
[51] W. Qiao and Z. Yang, "Solving large-scale function optimization problem by using a new metaheuristic algorithm based on quantum dolphin swarm algorithm," *IEEE Access*, vol. 7, pp. 138972–138989, 2019.

NAN ZHANG is currently a Lecturer with the Key Laboratory of Western Mines and Hazard Prevention, Ministry of Education of China, College of Energy Engineering, Xi'an University of Science and Technology, China.

His research interests are focused on stability and tightness analysis of salt caverns in bedded rock salt.

XILIN SHI is currently an Associate Professor with the State Key Laboratory of Geomechanics and Geotechnical Engineering, Institute of Rock and Soil Mechanics, Chinese Academy of Sciences, China.

His research interests are focused on underground gas storage (UGS) and underground strategic petroleum reserve (SPR).

YUN ZHANG is currently a Lecturer with the Key Laboratory of Western Mines and Hazard Prevention, Ministry of Education of China, College of Energy Engineering, Xi'an University of Science and Technology, China.

His research interests are focused on mechanical properties of deep earth rocks.

PENGFEI SHAN is currently a Lecturer with the Key Laboratory of Western Mines and Hazard Prevention, Ministry of Education of China, College of Energy Engineering, Xi'an University of Science and Technology, China

His research interests are focused on stability of roadway surrounding rock analysis.